Mechanism of the Reaction Catalyzed by Mandelate Racemase: Structure and Mechanistic Properties of the K166R Mutant†

Abraham T. Kallarakal, Bharati Mitra,‡ John W. Kozarich,§ and John A. Gerlt*,||

Department of Chemistry and Biochemistry, University of Maryland, College Park, Maryland 20742

James G. Clifton and Gregory A. Petsko*

Rosenstiel Center for Biomedical Sciences, Brandeis University, Waltham, Massachusetts 02254

George L. Kenyon

Department of Pharmaceutical Chemistry, School of Pharmacy, University of California, San Francisco, California 94143

Received August 25, 1994; Revised Manuscript Received November 15, 1994®

ABSTRACT: On the basis of the available high-resolution structures of mandelate racemase (MR) from *Pseudomonas putida* [Landro, J. A., Gerlt, J. A., Kozarich, J. W., Koo, C. W., Shah, V. J., Kenyon, G. L., Neidhart, D. J., Fujita, J., & Petsko, G. A. (1994) *Biochemistry 33*, 635−643], Lys 166 and His 297 are positioned appropriately to participate in catalysis as acid/base catalysts that either abstract the α-proton from the enantiomers of mandelate to form an enolic intermediate or protonate the enolic intermediate to form the enantiomers of mandelate, with Lys 166 participating as the (*S*)-specific acid/base catalyst and His 297 participating as the (*R*)-specific acid/base catalyst. In this paper we report the structural and mechanistic properties of the mutant in which Lys 166 has been replaced with arginine (K166R). The structure of K166R has been determined at 1.85 Å resolution with the substrate (*S*)-mandelate bound in the active site. The structure of this complex reveals no geometric alterations in the active site, with the exception that the longer side chain of Arg 166 is necessarily displaced upward from the position occupied by Lys 166 by steric interactions with the bound substrate. In contrast to the H297N mutant of MR [Landro, J. A., Kallarakal, A. T., Ransom, S. C., Gerlt, J. A., Kozarich, J. W., Neidhart, D. J., & Kenyon, G. L. (1991) *Biochemistry 30*, 9275−9281], the K166R exhibits low levels of racemase activity [k_{cat} is reduced 5×10^3-fold in the (*R*)- to (*S*)-direction and 1×10^3-fold in the (*S*)- to (*R*)-direction]. The substrate and solvent deuterium isotope effects support a reaction coordinate for the K166R-catalyzed reaction in which the transition state for interconversion of bound (*S*)-mandelate and the stabilized enolic intermediate is higher in energy that the transition state for interconversion of bound (*R*)-mandelate and the stabilized enolic intermediate. The solvent deuterium isotope effect when (*S*)-mandelate is substrate (2.2 ± 0.3) supports the proposal that the formation of the enolic intermediate involves partial transfer of a solvent-derived proton from Glu 317 to the substrate as the α-proton is abstracted [Mitra, B., Kallarakal, A. T., Kozarich, J. W., Gerlt, J. A., Clifton, J. G., Petsko, G. A., & Kenyon, G. L. (1995) *Biochemistry 34*, 2777−2787]. K166R catalyzes the stereospecific elimination of bromide ion from (*R*)-*p*-(bromomethyl)-mandelate to form *p*-(methyl)benzoylformate at a rate (0.012 s^{-1}) that is similar to that catalyzed by wild-type MR (0.025 s^{-1}) and H297N (0.012 s^{-1}), although the latter elimination is stereospecific for (*S*)-*p*-(bromomethyl)mandelate. The rate constant for the elimination reaction catalyzed by K166R suggests that the rate of interconversion of bound (*R*)-mandelate and the enolic intermediate is the same as that catalyzed by wild-type MR.

The equilibration of the (*R*)- and (*S*)-enantiomers of mandelate catalyzed by mandelate racemase (MR;[1] EC 5.1.2.2) from *Pseudomonas putida* ATCC 12633 is dependent upon two general acid−general base catalysts that transfer protons to and from the α-carbons of the substrate and product enantiomers: one abstracts the α-proton from the substrate enantiomer to form an enolic intermediate, and the second protonates the enolic intermediate to form the product enantiomer (Kenyon & Hegeman, 1979; Gerlt et al., 1992). These two catalysts have been identified as Lys 166 and His 297 on the basis of the high-resolution X-ray structure of wild-type MR (Neidhart et al., 1991; Landro et al., 1994). Lys 166 was appropriately positioned in the active site to act as the (*S*)-specific acid/base catalyst while His 297 was

† This is paper 19 in a series on mandelate racemase; paper 18 is Mitra et al. (preceding paper in this issue). This research was supported by Grant GM-40570 (J.A.G., G.L.K., J.W.K., and G.A.P.) from the National Institutes of Health.

‡ Present address: Department of Biochemistry, Wayne State University School of Medicine, Detroit, MI 48201.

§ Present address: Department of Biochemistry, Merck Research Laboratories, P.O. Box 2000, Rahway, NJ 07065-0900.

|| Present address: Department of Biochemistry, 415 Roger Adams Laboratory, University of Illinois, Urbana, IL 61801.

® Abstract published in *Advance ACS Abstracts,* February 1, 1995.

[1] Abbreviations: CHES, 2-(cyclohexylamino)-1-ethanesulfonic acid; HEPES, 4-(2-hydroxyethyl)piperazine-1-ethanesulfonic acid; LB, Luria broth; MES, 2-(*N*-morpholino)ethanesulfonic acid; MR, mandelate racemase; PIPES, piperazine-1,4-bis(2-ethanesulfonic acid); TAPS, *N*-[tris(hydroxymethyl)methyl]-3-aminopropanesulfonic acid.

0006-2960/95/0434-2788$09.00/0

appropriately positioned to act as the (*R*)-specific acid/base catalyst.

The stepwise nature of these proton transfer reactions was unequivocally established by mechanistic investigation of the structurally conservative H297N mutant (Landro et al., 1991). This mutant was inactive as a catalyst that equilibrates the (*R*)- and (*S*)-enantiomers of mandelate. However, the mutant was observed to catalyze a facile exchange of the α-proton of (*S*)- but not (*R*)-mandelate with D_2O solvent. These findings suggested that, in the absence of a general acidic catalyst (the imidazolium group of His 297) that can deliver a proton to generate (*R*)-mandelate, a transiently stable enolic intermediate can be formed by the abstraction of the α-proton from (*S*)-mandelate by the ϵ-amino group of Lys 166. During the lifetime of this enolic intermediate, rotation about the C−N bond of the ϵ-ammonium group of Lys 166 can occur, thereby allowing the enolic intermediate to be deuteriated by the ammonium group of Lys 166.

Wild-type MR catalyzes the elimination of bromide ion from both enantiomers of (*R,S*)-*p*-(bromomethyl)mandelate to form *p*-(methyl)benzoylformate (Lin et al., 1988). The 1,6-elimination of bromide ion is presumed to occur from an enolic intermediate that is formed by abstraction of the α-proton by Lys 166 [the (*S*)-enantiomer] or His 297 [the (*R*)-enantiomer]. This intermediate partitions between protonation and elimination of bromide ion. In contrast, the H297N mutant catalyzes the elimination of bromide ion from only the (*S*)-enantiomer of (*R,S*)-*p*-(bromomethyl)mandelate (Landro et al., 1991): the inert (*R*)-enantiomer accumulates as (*R*)-*p*-(hydroxymethyl)mandelate since the benzylic bromide is readily solvolyzed at neutral pH. The susceptibility of only the (*S*)-enantiomer to elimination can be explained if the ϵ-amino group of Lys 166 retains its ability to abstract the α-proton from the (*S*)-enantiomer, but the carboxamide group of Asn 297 that is in the position occupied by the imidazole functional group of His 297 in wild-type MR is unable to abstract the α-proton from the (*R*)-enantiomer.

This likely participation of the ϵ-amino group of Lys 166 in the racemization reaction catalyzed by wild-type MR was supported by the finding that it can be alkylated by the active site-directed affinity label α-phenylglycidate (Landro et al., 1994). The oxirane ring of the (*R*)-enantiomer of α-phenylglycidate is opened by nucleophilic attack of the ϵ-amino of Lys 166 on the unsubstituted carbon to yield the inactivated enzyme; this reaction may be catalyzed by the imidazolium group of His 297. The structural characterization of the alkylated, inactivated enzyme was accomplished by X-ray crystallography. The structure of the adduct revealed not only that the ϵ-amino group of Lys 166 had been alkylated but also the nature of the interaction of both the hydroxyl group formed by opening of the oxirane ring and the carboxylate group with the active site. The Mg^{2+} that is required both for catalytic activity and for the inactivation by α-phenylglycidate is coordinated to both the hydroxyl group and one of the carboxylate oxygens. The other carboxylate oxygen is hydrogen-bonded to the carboxylic acid functional group of Glu 317. The structure of this covalent adduct can be considered to be that of (*S*)-mandelate covalently linked to the ϵ-amino group of Lys 166 *via* a methylene bridge. Thus, since we have been unable to obtain cocrystals of either enantiomer of mandelate bound in the active site of wild-type MR, we assume that this structure may resemble that of (*S*)-mandelate bound in the active site. An analogous structure was solved for the competitive inhibitor (*S*)-atrolactate bound in the active site of wild-type MR, i.e., bidentate coordination of the Mg^{2+} with the hydroxyl group and one carboxylate oxygen and hydrogen bonding of the other carboxylate oxygen with the carboxylic acid functional group of Glu 317.

In this paper we describe the structural and mechanistic characterization of the K166R mutant of MR. A high-resolution X-ray structure of K166R has been obtained with (*S*)-mandelate bound in the active site; this is the first structure of MR in which an enantiomer of the substrate is bound in the active site. In contrast to the H297N mutant of MR (Landro et al., 1991), the K166R mutant retains a low level of racemase activity. K166R catalyzes the elimination of bromide ion from only the (*R*)-enantiomer of (*R,S*)-*p*-(bromomethyl)mandelate. This stereospecificity contrasts with that observed for the elimination of bromide ion catalyzed by the H297N mutant [which only utilized the corresponding (*S*)-enantiomer], suggesting that in K166R the imidazole group of His 297 retains the ability to abstract the α-proton from the substrate analog. These findings further support the proposal that both Lys 166 and His 297 function as acid/base catalysts in the reactions catalyzed by MR.

MATERIALS AND METHODS

Restriction endonucleases and polynucleotide kinase from bacteriophage T4 were purchased from New England Biolabs. DNA ligase from bacteriophage T4 and calf intestinal phosphatase were obtained from Boehringer Mannheim. Site-directed mutagenesis was performed by the phosphorothioate method with the kit purchased from Amersham. DNA sequence analysis were performed by use of the Sequenase kit supplied by U.S. Biochemicals. Synthetic oligonucleotides were purchased from the Protein Nucleic Acid Laboratory, University of Maryland, College Park. Standard techniques were employed for isolating plasmid DNA and DNA fragments, cloning and transformation, and resolving protein and DNA samples by electrophoresis (Sambrook et al., 1989).

The plasmids that direct the inducible synthesis of wild-type MR in *Escherichia coli*, pMRtrc/WT (Ransom et al., 1988), and the constitutive synthesis of MR in *Pseudomonas aeruginosa* ATCC 15692, pMRαpg (Tsou et al., 1989), have been described.

(*R,S*)-*p*-(Bromomethyl)mandelate was prepared according to the procedure described by Lin et al. (1988).

[α-^{2}H]-(*R*)-Mandelate was prepared by fractional recrystallization of diastereomeric salts of racemic [α-^{2}H]mandelic acid that was synthesized using wild-type MR to catalyze the exchange of substrate protium with solvent deuterium (Mitra et al., 1995).

[α-^{2}H]-(*S*)-Mandelate was synthesized from [α-^{1}H]-(*S*)-mandelate using H297N to catalyze the exchange of substrate protium with solvent deuterium (Landro et al., 1991).

Site-Directed Mutagenesis. The template for mutagenesis was M13mp18 into which the 1.9 kb *Eco*RV−*Sst*I fragment of pMRαpg (Tsou et al., 1989) containing the entire gene for MR had been cloned (Landro et al., 1991). The synthetic 22-mer d(GGTTAAGACCCGAATCGGCTAT) was used for constructing K166R substitution, where the position of the mutagenic mismatches are underlined. The entire mutant

Table 1: Data Collection Statistics from XSCALE

high-resolution limit (Å)	*R* factor (%) orientation 1	*R* factor (%) orientation 2	*R* factor (%) merging	completeness $I > 0\sigma$	completeness $I > 1\sigma$	completeness $I > 2\sigma$	completeness $I > 3\sigma$
6.00	4.5	4.5	4.5	93.2	90.8	89.5	88.5
4.50	4.7	4.8	4.8	97.9	94.1	92.0	90.3
3.00	6.7	6.2	6.4	97.9	92.3	88.7	85.6
2.50	15.6	13.6	14.4	97.0	92.1	84.8	75.4
2.10	23.2	21.2	22.0	94.7	90.6	81.8	68.7
1.95	32.9	27.0	29.0	86.3	83.4	73.7	59.2
1.84	43.4	32.3	35.8	70.1	66.8	55.6	40.2
total			11.0				

Table 2: *R*-Factor Report to 1.85 Å Resolution from TNT

data set	count	rejected by resolution	% completeness
observed	32 004	313	87
calculated	36 289		100

31 691 matches were found (87% complete)

Resolution limits: 20.0−1.85 Å

Bragg spacing (Å)	5.00	3.48	2.93	2.62	2.41	2.26	2.14	2.04	1.95	1.88	total
reflections	3591	3380	3375	3334	3315	3265	3216	3017	2786	2412	31691
R factor	0.17	0.14	0.17	0.18	0.17	0.18	0.19	0.21	0.24	0.28	0.184

gene was sequenced following mutagenesis by using a series of synthetic primers.

Purification of Enzymes from P. aeruginosa Transformed with pKTtrc/MR. The genes for both wild-type MR and K166R were expressed in *P. aeruginosa* ATCC 15692. The genes for wild-type MR or K166R together with the *trc* promoter were cloned into the broad-host range vector pKT230 as previously described (Landro et al., 1991). The plasmid containing the gene for K166R was designated pKTtrc/K166R. *P. aeruginosa* was then transformed with either pKTtrc/WT (Landro et al., 1991) or pKTtrc/K166R and grown in LB media supplemented with 1 mg/mL streptomycin. The purification of the proteins was carried out according to established protocols (Ransom et al., 1988). Since K166R had very low racemase activity, SDS−PAGE as well as enzyme assays was used to monitor column fractions for the K166R protein.

Crystallization of K166R. K166R was cocrystallized with the substrate (*R*)-mandelate by the hanging drop method using the procedure described in the previous paper (Mitra et al., 1995). Crystals appeared after 1−2 days and were fully grown after 1 week. Suitable single crystals were mounted in quartz capillary tubes directly from the hanging drop shortly before data collection.

Data Collection. All data were collected from a single crystal with Cu Kα X-rays using a Siemens multiwire detector mounted on a Elliot GX-6 rotating anode generator, operated with a fine-focus cup at approximately 30 kV and 30 mA. A cold air stream maintained the crystal temperature around 4 °C. Data frames were processed using the XDS program (Kabsch, 1988a,b). Two different orientations were collected and merged using the program XSCALE (Kabsch, 1988b). The space group and unit cell parameters were isomorphous to those of wild-type MR (*I*422; 125.32 × 125.32 × 106.42 Å). The merged 1.85 Å data set had an overall merging *R* factor of 11% on intensity. Based on the statistics of the merging *R* factor *vs* resolution and completeness *vs* signal to noise (σ), the final "working" data set contained 32 004 reflections to 1.85 Å resolution that have intensities greater than 1σ (Table 1).

Structure Refinement. Initial difference electron density maps calculated using these data and the phases from the refined structure of wild-type MR indicated that there were no gross structural rearrangements; all of the active site residues, including residue 166, fit cleanly into the electron density. Additionally, there was continuous density in the region where the substrate was expected to bind. The initial model for refinement was the wild-type structure, with residue 166 modeled as alanine (to debias the phases) and with neither water molecules nor the substrate present.

The program TNT (Tronrud et al., 1987; Tronrud, 1992) was used for least squares refinement of this model *vs* the observed structure amplitudes from the mutant. After refinement against increasingly higher resolution data, new difference electron density maps were calculated. Both the arginine side chain of residue 166 and the substrate could be placed unambiguously in the difference electron density and were added to the model. Although K166R was cocrystallized with (*R*)-mandelate, the (*S*)-enantiomer is bound in the active site. Further cycles of refinement after the addition of water molecules improved the electron density map to the point where a second substrate molecule, probably at lower occupancy, could be seen in the entrance to the active site; this molecule has the (*R*)-configuration.

The final structure has an *R* factor of 18.4% *vs* all data to 1.85 Å resolution with intensities greater than 1σ (Table 2). The geometry deviations are all below target values: the rms bond length deviation is 0.019 Å and the rms bond angle deviation is 3.1° (Table 3). This structure contains 2699 protein atoms, 22 substrate atoms, 1 magnesium atom, and 172 water molecules. The coordinates for this structure have been deposited in the Protein Data Bank at Brookhaven National Laboratories.

Assay of Mandelate Racemase Activity. Mandelate racemase activity was quantitated at 25 °C using either (*R*)- or (*S*)-mandelate as substrate with the circular dichroic assay described by Sharp et al. (1979). The reaction conditions were 0.1 M K-HEPES, pH 7.5, containing 3 mM $MgCl_2$. Values for k_{cat} and K_m were determined using the program HYPER (Cleland, 1979).

Table 3: Geometry Report from TNT

class	no.	rms deviation from ideal values
bond length	2782	0.019 Å
bond angle	3758	3.08°
torsion angle[a]	1644	23.92°
trigonal atom nonplanarity	60	0.020 Å
planar groups	406	0.021 Å
bad contacts	10	0.083 Å
thermal parameter correlation	2309	2.822 Å^2

[a] Torsion angles were not constrained during refinement.

The dependence of k_{cat} and K_m on pH using (*R*)- or (*S*)-mandelate was evaluated with 0.1 M buffers, pH 5.5−9.5, containing 3 mM $MgCl_2$. The buffers used were MES, pH 5.5, 6.0, and 6.5; PIPES, pH 7.0; HEPES, pH 7.5 and 8.0; TAPS, pH 8.5; and CHES, pH 9.0 and 9.5 (Landro et al., 1991). Substrate concentrations ranged from 0.25 to 10 mM. The estimated errors for the k_{cat} values were ±10%. The pK_a values described by the data were determined using the program BELL (Cleland, 1979).

Solvent and Substrate Isotope Effects. Solvent isotope effects on k_{cat} were determined by comparing the rates of racemization of (*R*)- and (*S*)-[α-^{1}H]mandelates in 0.1 M HEPES buffer containing 3 mM $MgCl_2$ in either H_2O, pH 7.5, or D_2O, pD 7.5. The rates of the reaction were determined at 1, 3, and 7 mM concentrations of substrates; values for k_{cat} were then determined with the program HYPER.

Substrate isotope effects on k_{cat} were similarly determined by comparing the rates of racemization of (*R*)- and (*S*)-[α-^{1}H]mandelates and (*R*)- and (*S*)-[α-^{2}H]mandelates in 0.1 M HEPES, pH 7.5, containing 3 mM $MgCl_2$.

Elimination of Bromide Ion from (R,S)-p-(Bromomethyl)-mandelate. The elimination of bromide ion from (*R,S*)-*p*-(bromomethyl)mandelate catalyzed by both wild-type MR and K166R was monitored with an Orion Model 811 pH meter equipped with an Orion Model 94-35 bromide electrode (Lin et al., 1988; Landro et al., 1991). The reactions were carried out with 7.8 mg of K166R or 8.7 mg of wild-type MR in 100 mM Na-MES, pH 6.0, containing 1 mM $Mg(NO_3)_2$ in a volume of 2 mL. Each reaction was initiated by adding the substituted mandelate to a final concentration of 1 mM. A control experiment was performed without any enzyme to obtain the rate of nonenzymatic elimination of bromide ion.

In a separate experiment, an analogous reaction was performed with 37.5 mg of K166R in a total volume of 6.0 mL. The reaction was initiated by the addition of the racemic substituted mandelate to a final concentration of 1 mM. At 4, 5, and 6 min after the initiation of the reaction, 2-mL aliquots were withdrawn and quenched by the addition of HCl to a final concentration of 0.6 M. The precipitated protein was removed by centrifugation, and any remaining K166R was removed by filtration through a Centricon 30 filter. The deproteinized solutions were then chromatographed by multiple injections on a Beckman Ultrasphere ODS HPLC column (4.6 × 25 cm) with a mobile phase of 0.5% phosphoric acid/25% methanol at a flow rate of 1 mL/min. The effluent was monitored at 254 nm. The fractions containing *p*-(methyl)benzoylformate (**1**) (λ_{max} = 264 nm, ϵ = 14 400 M^{-1} cm^{-1}) and *p*-(hydroxymethyl)mandelate (**2**) (λ_{max} = 222 nm, ϵ = 7050 M^{-1} cm^{-1}) were combined separately. The isolated amounts of **1** and **2** for the three aliquots were 4 min, 0.75 μmol of **1**, 0.96 μmol of **2**, total recovery 86%; 5 min, 0.75 μmol of **1**, 0.79 μmol of **2**, total recovery 77%; and 6 min, 0.74 μmol of **1**, 0.73 μmol of **2**, total recovery 74%.

Circular Dichroism of p-(Hydroxymethyl)mandelates. The *p*-(hydroxymethyl)mandelate isolated from each time point was extracted into diethyl ether. The solvent was removed by rotary evaporation, and the residue was dissolved in ethanol. The molar ellipticities of 0.072 mM solutions of the *p*-(hydroxymethyl)mandelates in hexane/2-propanol (1:1) were calculated from circular dichroic spectra measured with a JASCO J-500C spectropolarimeter equipped with a JASCO DP-500N data processor. The circular dichroic spectra of authentic samples of 0.072 mM (*R*)-*p*-(hydroxymethyl)mandelate (Landro et al., 1991) and 0.072 mM (*R,S*)-*p*-(hydroxymethyl)mandelate (Landro et al., 1991) were also recorded.

RESULTS AND DISCUSSION

The experiments described in this paper were designed to probe further the importance of Lys 166 as an acid/base catalyst in the reaction catalyzed by MR. While the ε-amino group of Lys 166 has been shown to be reactive as a nucleophile in the irreversible inhibition of wild-type MR by α-phenylglycidate (Landro et al., 1994), we sought evidence using site-directed replacements for Lys 166 that this residue is, in fact, essential for the racemization reaction. We previously used such an approach to implicate His 297 as an acid/base catalyst (Landro et al., 1991). While the K166A, K166Q, and K166M substitutions have been constructed and are all inactive as racemases, they are also inactive in catalyzing the elimination of bromide ion from (*R,S*)-*p*-(bromomethyl)mandelate (A. T. Kallarakal and J. A. Gerlt, unpublished data). Since our previous studies implicated His 297 as an acid/base catalyst (Landro et al., 1991), we hypothesized that mutant enzymes containing a substitution for Lys 166 but retaining His 297 should be inactive as racemases but retain the ability to catalyze the elimination of bromide ion from (*R*)-*p*-(bromomethyl)mandelate, assuming that the substitution did not alter the structure of the active site. Since these mutants did not catalyze the elimination of bromide ion from (*R,S*)-*p*-(bromomethyl)mandelate, we assumed that these substitutions did alter the structure of the active site and, therefore, constructed the K166R substitution. As described in this paper, this mutant does retain the ability to catalyze the facile elimination of bromide ion from (*R*)-*p*-(bromomethyl)mandelate.

Structural Characterization of K166R. The K166R mutant of MR was constructed and purified to apparent homogeneity as described in the Materials and Methods section. The mutant enzyme was crystallized in the presence of (*R*)-mandelate and $(NH_4)_2SO_4$. The structure was solved to 1.85 Å resolution by difference Fourier analysis relative to the structure of wild-type MR refined to 2.0 Å resolution (Neidhart, 1993).

Although K166R was cocrystallized in the presence of (*R*)-mandelate, (*S*)-mandelate was observed in the active site. Although this was initially surprising, we explain the preferential binding of the (*S*)-enantiomer at pH ~5.8 by considering the dependencies of both k_{cat} and K_m on pH. As described in the next section, the dependencies of the kinetic

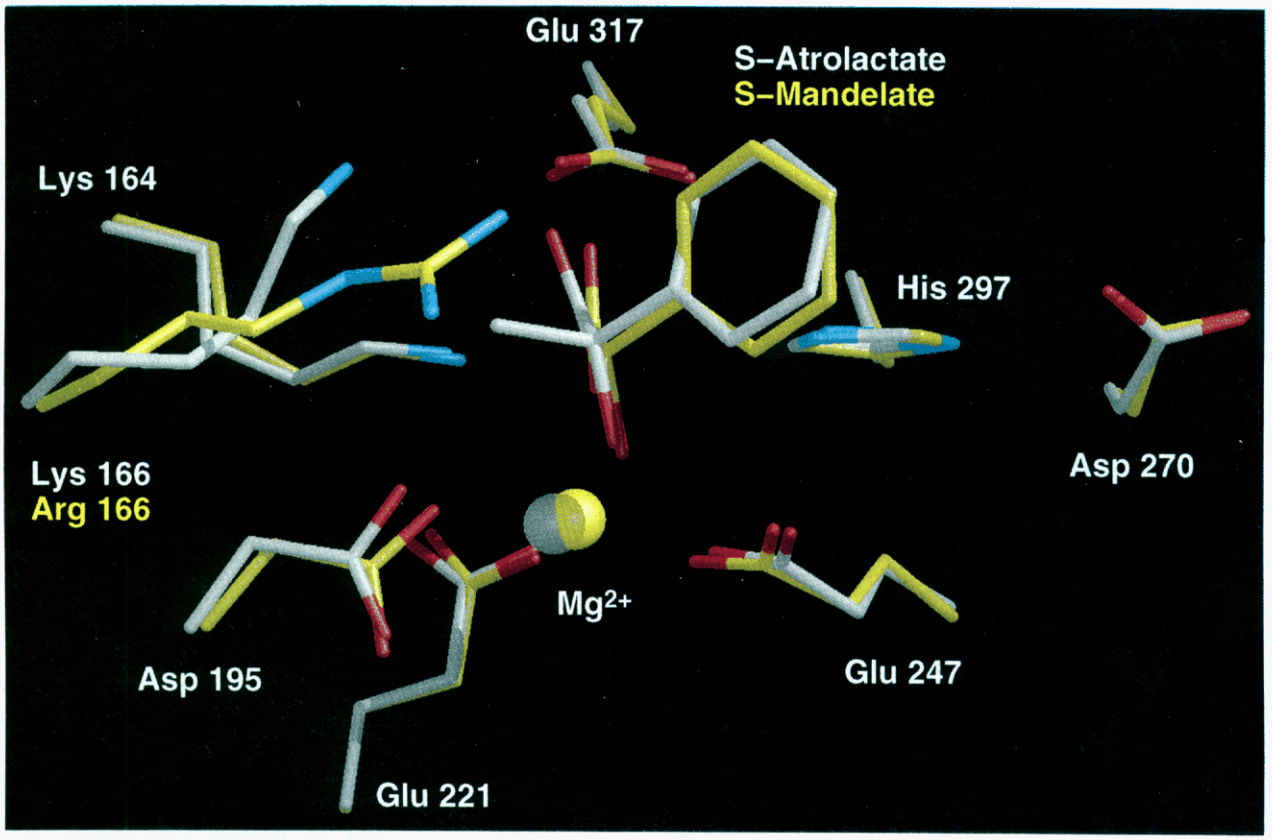

FIGURE 1: Superpositioning of the X-ray structures of the active site of wild-type MR with (*S*)-atrolactate bound in the active site (white; Landro et al., 1994) and of K166R with (*S*)-mandelate bound in the active site (yellow). See the text for experimental details.

parameters on pH for K166R differ from those measured for wild-type MR. For wild-type MR, the K_ms (and the k_{cat}s) for the enantiomers of mandelate have similar dependencies on pH from pH 5.5 to pH 10.5. However, for K166R, at pH values below 8.5, the K_m for (*S*)-mandelate is less than that for the (*R*)-enantiomer (with corresponding differences in the k_{cat}s so that the Haldane relationship is obeyed). Accordingly, the (*S*)-enantiomer should be preferentially bound under the conditions of crystallization.

A comparison of the overall active site structures for wild-type MR complexed with the competitive inhibitor (*S*)-atrolactate (white structure, Figure 1; Landro et al., 1994) and K166R complexed with the *substrate* (*S*)-mandelate (yellow structure, Figure 1) reveals no significant differences in active site geometry with the exception of the side-chain geometries of residues 166: (1) in the complex of wild-type MR with (*S*)-atrolactate, the α-methyl group of the inhibitor displaces the ϵ-amino group of Lys 166 upward from the position that it presumably would occupy if (*S*)-mandelate were bound in the active site; and (2) in the complex of K166R with (*S*)-mandelate, the substrate displaces the functional group of Arg 166 upward since the side chain of arginine is longer than that of lysine. We also note that the α-proton of the bound substrate is not in the plane of the guanidine/guanidinium functional group of Arg 166; i.e., the geometry is not amenable for facile transfer of a proton between substrate, the enolic intermediate, and the functional group of Arg 166 (*vide supra*). The functional group of His 297 in the active site of K166R is in the same position as the functional group of His 297 in the active site of wild-type MR. The distance between the α-carbon of (*S*)-mandelate and the ϵ-nitrogen of His 297 in the active site of K166R, 3.9 Å, does not allow the state of protonation of the

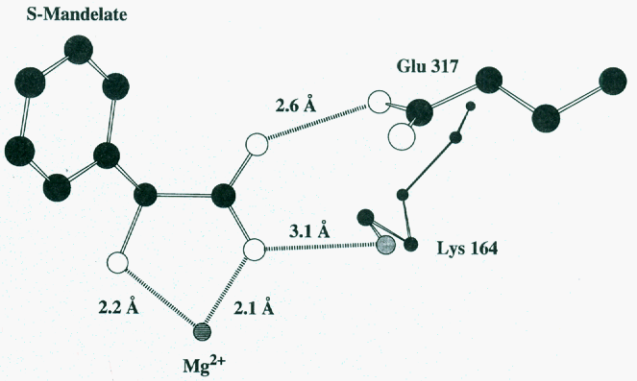

FIGURE 2: Interaction of (*S*)-mandelate with Mg^{2+} and the functional groups of Lys 164 and Glu 317 in the active site of K166R.

functional group of Arg 166 to be unequivocally specified. [Similar distances between the α-carbon of (*S*)-mandelate and the ϵ-nitrogen of His 297 are observed in the active sites of wild-type MR complexed with (*S*)-atrolactate (3.9 Å; Landro et al., 1994), E317Q complexed with (*S*)-atrolactate (3.8 Å; Mitra et al., 1995), and wild-type MR inactivated with α-phenylglycidate (3.8 Å; Landro et al., 1994).]

We have been unable to obtain a high-resolution structure of wild-type MR complexed with either enantiomer of mandelate, presumably because of the disorder caused by the rapid equilibration of the diastereomeric complexes with the substrate enantiomers.

(*S*)-Mandelate is coordinated to the essential Mg^{2+} in the active site of K166R (Figure 2) by both its hydroxyl group (2.1 Å) and one of its carboxylate oxygens (2.2 Å). The carboxylate oxygen of the inhibitor that is coordinated to Mg^{2+} is also hydrogen-bonded to the ϵ-ammonium group

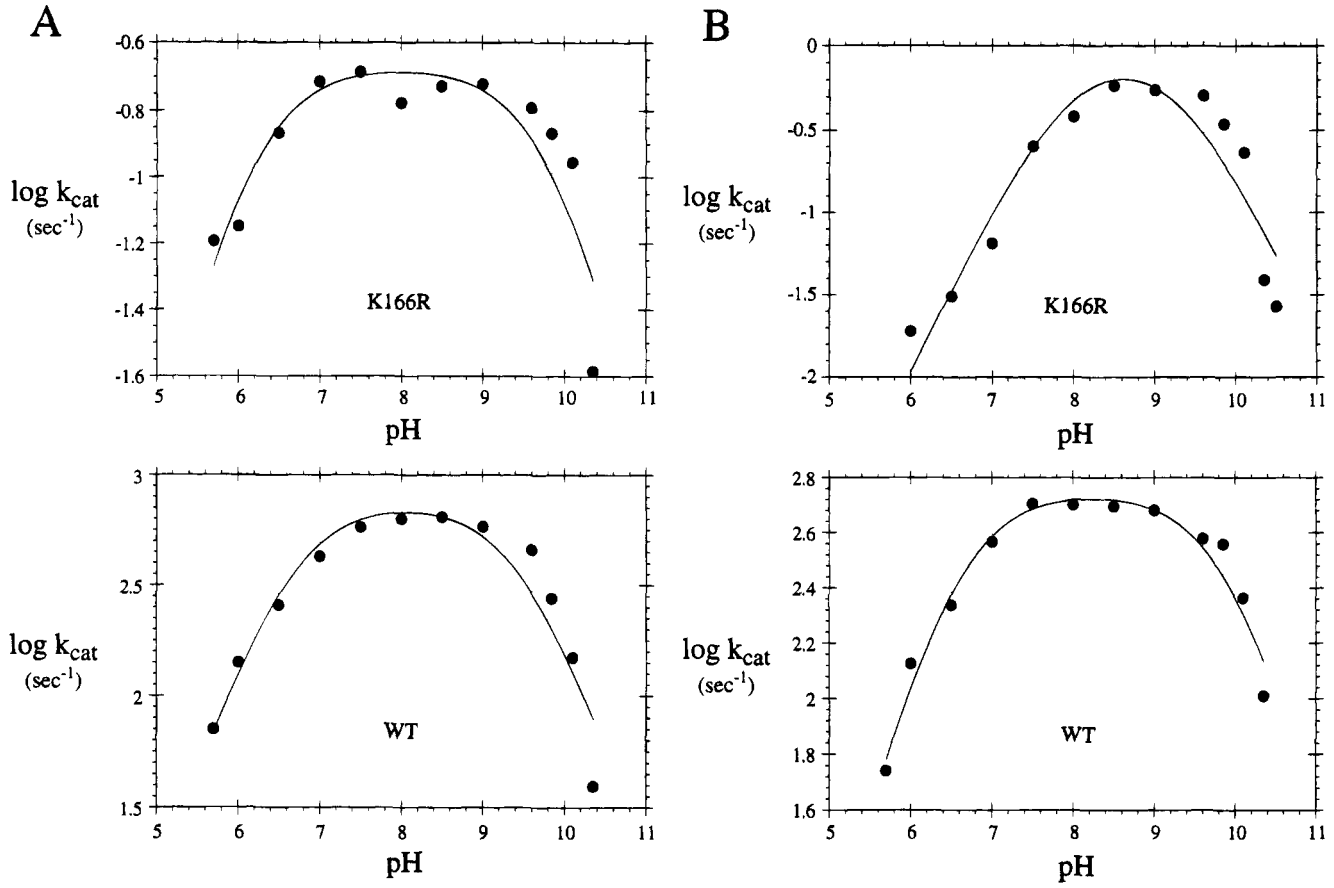

FIGURE 3: Dependence of k_{cat} on pH for K166R using (*R*)-mandelate (panel A) and (*S*)-mandelate (panel B) as substrate. See text for details.

of Lys 164 (3.1 Å) in the active site of K166R. Within the estimated errors, these distances are identical to those observed for wild-type MR complexed with (*S*)-atrolactate (Landro et al., 1994). Thus, neutralization of the negative charge of the carboxylate group of the bound inhibitor, and, by analogy, substrate, should be preserved in the K166R mutant.

The carboxylic acid group of Glu 317 both functions as a general acid catalyst that transfers a proton toward the carboxylic group of the substrate as the α-proton is abstracted and stabilizes the resulting enolic intermediate by participating in a short, strong hydrogen bond to the OH group of the intermediate (Mitra et al., 1995). In the active site of K166R (Figure 2), the carboxylate oxygen of (*S*)-mandelate that is not coordinated to the essential Mg^{2+} is hydrogen-bonded to the carboxylic acid group of Glu 317, as judged by the O−O distance between the bound substrate and the functional group (2.6 Å). Within error, this distance is identical to that observed for the analogous hydrogen bond involving the carboxylic acid group of Glu 317 in the active site of wild-type MR (2.8 Å; Landro et al., 1994).

Thus, the only observable difference in the active site of K166R relative to wild-type MR is the substitution of the arginine side chain with its guanidinium functional group for the lysine side chain with its ε-ammonium group at residue 166. As a result, any changes in catalytic activity can be associated with the Lys to Arg substitution at residue 166.

Mandelate Racemase Activity of K166R. The values for k_{cat} and K_m measured for K166R at pH 7.5 are compared to those measured for wild-type MR at pH 7.5 in Table 4. With

Table 4: Kinetic Constants for Wild-Type MR and K166R[a]

enzyme	k_{cat} (*R*) → (*S*) (s^{-1})	K_m (*R*) → (*S*) (mM)	k_{cat} (*S*) → (*R*) (s^{-1})	K_m (*R*) → (*S*) (mM)
wild type	480 ± 27	0.34 ± 0.06	440 ± 23	0.35 ± 0.09
K166R	0.21 ± 0.01	0.59 ± 0.12	0.46 ± 0.02	1.40 ± 0.10

[a] Assay methods are described in the Materials and Methods section.

either enantiomer of mandelate as substrate, the values for k_{cat} for K166R are reduced ≥1000-fold from the values for wild-type MR. The values for K_m are elevated 2−5-fold, with the net effect being that k_{cat}/K_m is reduced by a factor of ~5000 by the lysine to arginine substitution at residue 166.

The dependence of k_{cat} on pH using each enantiomer of mandelate as substrate is shown in Figure 3 [panel A, (*R*)-mandelate substrate; panel B, (*S*)-mandelate substrate]. For (*R*)-mandelate as substrate, the data for K166R can be described by a pK_a of 6.2 ± 0.1 for the ascending limb and a pK_a of 9.8 ± 0.2 for the descending limb; the limiting value for k_{cat} is 0.21 ± 0.03 s^{-1}. For (*S*)-mandelate as substrate, the data for K166R are described by a pK_a of 7.9 ± 0.3 for the ascending limb and a pK_a of 9.3 ± 0.3 for the descending limb; the limiting value for k_{cat} is 0.93 ± 0.46 s^{-1}. Since the data for (*S*)-mandelate as substrate do not clearly define a pH-independent range for k_{cat}, the pK_a for the ascending limb may be greater and/or the pK_a for the descending limb may be somewhat less than these calculated values. For wild-type enzyme, the dependencies of k_{cat} on pH are indistinguishable for the two enantiomers of mandelate (Figure 3), with a pK_a of ~6.4 describing the ascending limbs

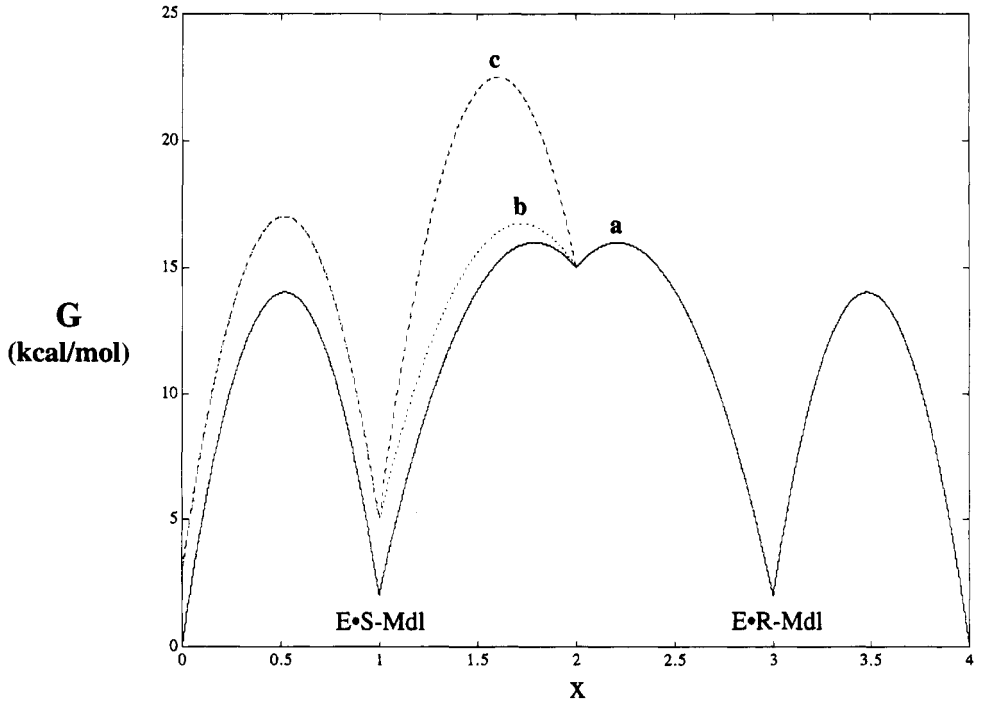

FIGURE 4: Dependence of G on the position of the reaction coordinate, x, for racemization of mandelate by MR. Free enzyme and (*S*)-mandelate are at $x = 0$, bound (*R*)-mandelate is at $x = 1$, bound enolic intermediate is at $x = 2$, bound (*R*)-mandelate is at $x = 3$, and free enzyme and (*R*)-mandelate are at $x = 4$. Reaction coordinates are generated with eq 1 for an inverted parabola, where ΔG° is the

$$G = -4\Delta G^{\ddagger}_{int}(x - 0.5)^2 + \Delta G^\circ(x - 0.5) \quad (1)$$

thermodynamic barrier and $\Delta G^{\ddagger}_{int}$ is the intrinsic kinetic barrier for each reaction. Reaction coordinate a (wild-type MR; solid line) was calculated assuming $\Delta G^\circ_{(0\rightarrow1)} = 2$ kcal/mol and $\Delta G^{\ddagger}_{int(0\rightarrow1)} = 13$ kcal/mol, $\Delta G^\circ_{(1\rightarrow2)} = 13$ kcal/mol and $\Delta G^{\ddagger}_{int(1\rightarrow2)} = 5.62$ kcal/mol, $\Delta G^\circ_{(2\rightarrow3)} = -13$ kcal/mol and $\Delta G^{\ddagger}_{int(2\rightarrow3)} = 5.62$ kcal/mol, and $\Delta G^\circ_{(3\rightarrow4)} = -2$ kcal/mol and $\Delta G^{\ddagger}_{int(3\rightarrow4)} = 13$ kcal/mol. Reaction coordinate b (dotted line) was calculated assuming $\Delta G^\circ_{(0\rightarrow1)} = 2$ kcal/mol and $\Delta G^{\ddagger}_{int(0\rightarrow1)} = 13$ kcal/mol, $\Delta G^\circ_{(1\rightarrow2)} = 10$ kcal/mol and $\Delta G^{\ddagger}_{int(1\rightarrow2)} = 5.62$ kcal/mol, $\Delta G^\circ_{(2\rightarrow3)} = -13$ kcal/mol and $\Delta G^{\ddagger}_{int(2\rightarrow3)} = 5.62$ kcal/mol, and $\Delta G^\circ_{(3\rightarrow4)} = -2$ kcal/mol and $\Delta G^{\ddagger}_{int(3\rightarrow4)} = 13$ kcal/mol. Reaction coordinate c (K166R; dashed line) was calculated assuming $\Delta G^\circ_{(0\rightarrow1)} = 2$ kcal/mol and $\Delta G^{\ddagger}_{int(0\rightarrow1)} = 13$ kcal/mol, $\Delta G^\circ_{(1\rightarrow2)} = 10$ kcal/mol and $\Delta G^{\ddagger}_{int(1\rightarrow2)} = 12$ kcal/mol, $\Delta G^\circ_{(2\rightarrow3)} = -13$ kcal/mol and $\Delta G^{\ddagger}_{int(2\rightarrow3)} = 5.62$ kcal/mol, and $\Delta G^\circ_{(3\rightarrow4)} = -2$ kcal/mol and $\Delta G^{\ddagger}_{int(3\rightarrow4)} = 13$ kcal/mol. For reaction coordinate a, the values of G are normalized so that $G = 0$ when $x = 0$; for reaction coordinates b and c, the values of G are normalized so that $G = 3$ kcal/mol (~2 pK_a units) when $x = 0$. For reaction coordinate a, this normalization was accomplished by adding the value of G when $x = 0$ ($\Delta G^{\ddagger}_{int} + \Delta G^\circ/2$) to the value of G calculated with eq 1. For reaction coordinates b and c, the normalization was accomplished by adding the value of G when $x = 0$ ($\Delta G^{\ddagger}_{int} + \Delta G^\circ/2 + 3$ kcal/mol) to the value of G calculated with eq 1. The reaction coordinates were calculated and plotted with Macintosh MATLAB 3.5, The Mathworks, Inc., Natick, MA.

and a pK_a of 10.0 describing the descending limbs (Landro et al., 1991). Within the estimated errors, the effect of the K166R substitution is to increase the pK_a for the ascending limb when (*S*)-mandelate is substrate by ≥1.5 pK_a (as well as to reduce k_{cat}).

This increase in the pK_a of the ascending limb when (*S*)-mandelate is substrate is in qualitative accord with our earlier assignment of this pK_a to the necessary deprotonation of the conjugate acid of the active site general basic catalyst that abstracts the α-proton from the substrate to generate the enolic intermediate. Since the pK_a of the guanidinium group of arginine in solution is ~12.5 while that of the ϵ-ammonium group of lysine is ~10.5 (Creighton, 1993), we could expect an increase of ~2 pK_a units if a pK_a in the pH−rate profile is associated with the ϵ-ammonium group of a lysine residue in wild-type MR and the guanidinium group of an arginine residue in K166R. We note, however, that the pK_as of the descending limbs do not appear to be significantly altered by the K166R substitution. This suggests that our earlier tentative assignment of the pK_as of the descending limbs to the deprotonation of the active site general acidic catalyst that delivers a proton to the enolic intermediate to generate the product enantiomer may be incorrect. The assignments of ionizable groups responsible for the pK_as observed in the ascending and descending limbs of the dependence of k_{cat} on pH remain under investigation.

Free Energy Profiles for Wild-Type MR and K166R. What are the expected consequences of the K166R substitution on the reaction (free energy) profile? We base our answers to this question on the analysis recently presented by Gerlt and Gassman (1993a,b) for understanding the rates of abstraction of the α-protons of carbon acids in enzyme active sites.

The K166R substitution is expected to alter the internal thermodynamics of the reaction coordinate as compared to the reaction coordinate for wild-type MR (Figure 4). In wild-type MR the available evidence indicates that the pK_as of the ϵ-ammonium group of Lys 166 and the imidazolium group of His 297 are equivalent (Landro et al., 1991). Thus, the form of wild-type MR that binds (*S*)-mandelate (Lys 166 deprotonated, His 297 protonated) and the form that binds (*R*)-mandelate (Lys 166 protonated, His 297 deprotonated) are expected to be isoenergetic. This expectation is supported by the observation that the K_ms for (*R*)- and (*S*)-mandelates are similar (Whitman et al., 1985; Mitra et al., 1995). In contrast, since the pK_a of Arg 166 appears to

exceed that of His 297 by ≥1.5 p*K*a units (*vide supra*), the form of the enzyme that binds (*S*)-mandelate (Arg 166 deprotonated, His 297 protonated) will be destabilized relative to the form of the enzyme that binds (*R*)-mandelate (Arg 166 protonated, His 297 deprotonated). In qualitative accord with this prediction, the K_m of K166R for (*S*)-mandelate is ~2.5-fold greater than that for (*R*)-mandelate. However, this effect is not expected to decrease k_{cat} for the racemization reactions catalyzed by K166R, since the destabilization of the form of the enzyme that binds (*S*)-mandelate is expected to decrease the thermodynamic barrier, $\Delta G°$, for formation of the enolic intermediate: the difference between the pK_as of the α-proton in the transition state and the basic guanidine group of Arg 166 should be less than the difference between the pK_as between the α-proton in the transition state and the ϵ-amino group of Lys 166 in wild-type MR. [That the observed effect on the K_ms is less than that predicted on the basis of the pK_as may reflect destabilization of the form that binds (*R*)-mandelate (Arg 166 protonated, His 297 deprotonated) by unfavorable steric interactions between the phenyl ring in (*R*)-mandelate and the functional group of Arg 166 (see Figure 1)].

The predicted reaction coordinates for the reactions catalyzed by wild-type MR and K166R are shown in Figure 4. Although the reaction catalyzed by wild-type MR involves the formation of a stabilized enolic intermediate, the concentration of this intermediate has not yet been determined. On the basis of the analysis presented by Gerlt and Gassman (1993a,b), we assume that the concentration of the enolic intermediate will be small relative to the concentrations of bound substrates. Thus, we propose that the reaction catalyzed by wild-type MR can be described by reaction coordinate a in Figure 4.

At the pH optimum for the K166R mutant, the form of the enzyme that binds (*S*)-mandelate (Arg 166 deprotonated, His 297 protonated) is destabilized relative to the form that binds (*R*)-mandelate (Arg 166 protonated, His 297 deprotonated). However, since this destabilization will make the transfer of the α-proton from (*S*)-mandelate more favorable by the amount of the destabilization, the enolic intermediate is expected to be isoenergetic with the enolic intermediate in the reaction catalyzed by wild-type MR. This effect is described by reaction coordinate b in Figure 4. From inspection of this profile, the thermodynamic barrier, $\Delta G°$, for formation of the enolic intermediate from (*S*)-mandelate in the active site of K166R, i.e., the difference between the pK_as of the α-proton in the transition state and the basic guanidine group of Arg 166, should be less than $\Delta G°$ for formation of the enolic intermediate from (*R*)-mandelate in the active site of K166R (or from either enantiomer of mandelate in the active site of wild-type MR). Thus, other factors must be responsible for the observed $\geq 10^3$-fold decreases in the k_{cat}s for the racemization reactions catalyzed by K166R.

Since the side chain of arginine is longer than that of lysine, the position that its functional group occupies in the active site of K166R is not expected to be identical to that occupied by the functional group of Lys 166 in the active site of wild-type MR. As noted previously, the crystal structure of the complex of K166R with (*S*)-mandelate reveals that the α-proton of the substrate is not in the plane of the functional group of Arg 166 (Figure 1). Since this geometry is not expected to be favorable for facile proton transfer reactions, the observed decrease in k_{cat} accompanying the K166R substitution can be explained. In terms of the analysis presented by Gerlt and Gassman (1993a,b), this orientation effect is expected to increase the intrinsic kinetic barrier, $\Delta G^{\ddagger}_{int}$, for the proton transfer reactions between (*S*)-mandelate, the enolic intermediate, and the functional group of Arg 166. By definition, $\Delta G^{\ddagger}_{int}$ is a measure of the instability of the transition state in an isoergonic reaction. Thus, an unfavorable orientation between the functional group of Arg 166 and the substrate/enolic intermediate will increase $\Delta G^{\ddagger}_{int}$ and decrease the rate of the proton transfer reaction, even though $\Delta G°$ for the proton transfer reaction should not be affected by the unfavorable orientation between the reacting centers. While the magnitude of the increase in $\Delta G^{\ddagger}_{int}$ resulting from the position of the general basic functional group of Arg 166 cannot be quantitatively predicted, as shown in reaction coordiate c in Figure 4, the observed decrease in k_{cat} can be described by an increase in $\Delta G^{\ddagger}_{int}$ of ~6 kcal/mol.

From inspection of reaction coordinate c in Figure 4, we note that from this analysis the effects of the K166R substitution are predicted to be restricted to those reactions involving (*S*)-mandelate, i.e., the binding of (*S*)-mandelate and the interconversion of bound (*S*)-mandelate and enolic intermediate.

Solvent and Substrate Isotope Effects. The predicted reaction coordinate for the reaction catalyzed by K166R (reaction coordinate c, Figure 4) can be qualitatively examined by measuring solvent and substrate deuterium isotope effects on k_{cat}. In the (*S*)- to (*R*)-direction, formation of the enolic intermediate by abstraction of the α-proton from the substrate by the general basic guanidine group of Arg 166 is predicted to be the major determinant of k_{cat}. In the (*R*)- to (*S*)-direction, protonation of the enolic intermediate with a solvent-derived proton from the general acidic guanidinium group of Arg 166 is predicted to be the major determinant of k_{cat}.

In the (*S*)- to (*R*)-direction, the transition state for formation of the enolic intermediate from bound substrate involves not only abstraction of the α-proton from the substrate by the general basic guanidine group of Arg 166 but also proton transfer from Glu 317 toward the carboxylic acid group of the bound substrate in the formation of the enolic intermediate (Gerlt & Gassman, 1993a,b; Mitra et al., 1995). We have proposed that the enolic intermediate is stabilized by a short, strong hydrogen bond between the carboxylate group of Glu 317 and the enol tautomer of mandelic acid; in such hydrogen bonds, the proton is equally shared by both the carboxylate group and the enolic intermediate (Gerlt & Gassman, 1993a,b; Mitra et al., 1995). Although the solvent-derived proton remains partially bonded to the donor carboxylate group, its fractionation factor should be decreased so its partial transfer from Glu 317 to the enolic intermediate is expected to be accompanied by a solvent deuterium isotope effect (Gerlt & Gassman, 1993a,b). The abstraction of the α-proton can be detected by a substrate deuterium isotope effect; the proton transfer between Glu 317 and the enolic intermediate can be detected by a solvent deuterium isotope effect. Accordingly, we predict that both the substrate and solvent deuterium isotope effects should be greater than unity in the (*S*)- to (*R*)-direction.

In the (*R*)- to (*S*)-direction, the transition state for protonation of the enolic intermediate involves not only

proton transfer from the general acidic guanidinium group of Arg 166 but also proton transfer from the enolic intermediate toward Glu 317. While the protonation of the enolic intermediate by Arg 166 is expected to be subject to a large solvent deuterium isotope effect, the transfer of a solvent-derived proton from the enolic intermediate to the carboxylate group of Glu 317 may not be subject to a large deuterium isotope effect (Gerlt & Gassman, 1993a,b). The observed solvent deuterium isotope effect will be a composite of both of these effects, so assignment of values to the component effects is not possible. Since the formation of (*S*)-mandelate from the enolic intermediate does not involve transfer of a substrate-derived proton, the substrate deuterium isotope effect should be negligible (i.e., unity). Accordingly, we predict that only the solvent deuterium isotope effect should be greater than unity in the (*R*)- to (*S*)-direction.

These predictions have been experimentally verified. In the (*S*)- to (*R*)-direction, both the substrate and solvent deuterium isotope effects are greater than unity (3.6 ± 0.2 and 2.2 ± 0.3, respectively). In the (*R*)- to (*S*)-direction, the solvent deuterium isotope effect is greater than unity (3.4 ± 0.2) but the substrate deuterium isotope effect is indistinguishable from unity (1.1 ± 0.1).

We conclude that the substrate and solvent isotope effects for the racemization reactions catalyzed by K166R confirm both the predicted asymmetry of the reaction coordinate for the reaction catalyzed by K166R (reaction profile c in Figure 4) and, more importantly, the proposal that *concerted partial* transfer of a proton from the carboxylic acid functional group of Glu 317 to the carboxylate group of the substrate [either (*S*)- or (*R*)-mandelate] is required for abstraction of the α-proton by the general basic catalyst (Gerlt & Gassman, 1993a,b).

Elimination of Bromide Ion from (R,S)-p-(Bromomethyl)-mandelate. Wild-type MR catalyzes elimination of bromide ion from both enantiomers of (*R,S*)-*p*-(bromomethyl)mandelate to yield *p*-(methyl)benzoylformate. The H297N mutant of MR catalyzes the stereospecific elimination of bromide ion from (*S*)-*p*-(bromomethyl)mandelate but at a rate that is approximately one-half that observed for wild-type MR (Lin et al., 1988; Landro et al., 1991; A. T. Kallarakal and J. A. Gerlt, unpublished observations). The stereospecificity observed in this latter reaction was used as evidence that His 297 is an essential general basic catalyst and that in the active site of H297N the ϵ-amino group of Lys 166 retained its ability to act as a general basic catalyst.

We have studied both the rate and stereospecificity of the elimination of bromide ion from (*R,S*)-*p*-(bromomethyl)-mandelate catalyzed by K166R. As shown in Figure 5, K166R catalyzes the rapid elimination of bromide ion from approximately one-half of the racemic mixture of the substituted mandelate. After 5 min, the observed slow release of bromide ion is that associated with solvolysis of the inert enantiomer of *p*-(bromomethyl)mandelate to form *p*-(hydroxymethyl)mandelate. The rate of the enzyme-catalyzed elimination reaction is 0.012 s^{-1}. This rate is equal to that measured for the elimination of bromide ion catalyzed by H297 and approximately one-half that observed for wild-type MR (Lin et al., 1988; Landro et al., 1991; A. T. Kallarakal and J. A. Gerlt, unpublished observations). Thus, the elimination of bromide ion from *p*-(bromomethyl)-mandelate catalyzed by K166R appears to be stereospecific.

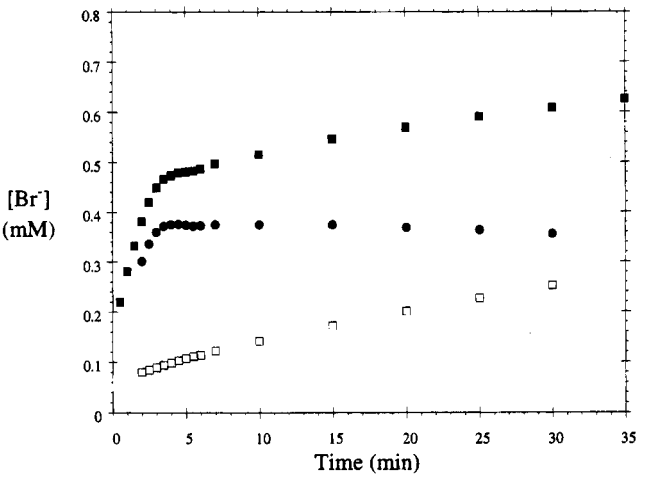

FIGURE 5: Time dependence of the elimination of bromide ion from (*R,S*)-*p*-(bromomethyl)mandelates catalyzed by K166R. Symbols: total bromide ion released, ■; nonenzyme-catalyzed bromide ion release, □; enzyme-catalyzed bromide ion release, ●.

That the rate of bromide ion elimination catalyzed by K166R is, within a factor of 2, equal to that of wild-type MR supports the assumptions used to construct reaction coordinate c in Figure 4; i.e., the Lys to Arg substitution alters neither the ΔG° nor the $\Delta G^\ddagger$ for formation of the enolic intermediate from the (*R*)-enantiomer of bound substrate.

The absolute configuration of the inert enantiomer of *p*-(bromomethyl)mandelate was determined by quenching aliquots of the reaction at 4, 5, and 6 min after the reaction was initiated, i.e., as soon as the enzyme-catalyzed elimination reaction was complete. Unlike H297N (Landro et al., 1991), K166R retains a small amount of racemase activity (*vide infra*) so the configuration of the inert enantiomer would be racemized if the reaction were not promptly quenched after the enzyme-catalyzed phase is complete. [In the analogous studies performed with H297N (Landro et al., 1991), the configuration of the inert enantiomer could be determined after the nonenzymatic elimination of bromide ion was also complete.] The configuration of the inert enantiomer was determined for each aliquot as described in the Materials and Methods section.

The circular dichroic spectra that were obtained for equal concentrations (0.072 mM) of authentic (*R*)-*p*-(hydroxymethyl)mandelate (spectrum A), the product of the K166R-catalyzed reaction after 5 min (spectrum B), and racemic *p*-(hydroxymethyl)mandelate (spectrum C) are shown in Figure 6. From inspection of these spectra, the inert enantiomer of *p*-(bromomethyl)mandelate has the (*S*)-configuration, indicating that K166R catalyzes the stereospecific elimination of bromide ion from (*R*)-*p*-(bromomethyl)-mandelate. The enantiomeric excess of the *p*-(hydroxymethyl)mandelate isolated from the K166R-catalyzed reaction is 37.7%. The enantiomeric excesses of the (*R*)-*p*-(hydroxymethyl)mandelate isolated from the aliquots removed 4 and 6 min after the reaction was initiated were less, 30.4% and 10.9%, respectively (data not shown). In the earlier aliquot, the enzyme-catalyzed elimination reaction apparently was not complete, and in the later aliquot, enzyme-catalyzed racemization was apparently significant. Therefore, the result is secure that the stereospecificity of the elimination reaction catalyzed by K166R is opposite that observed for the elimination reaction catalyzed by H297N.

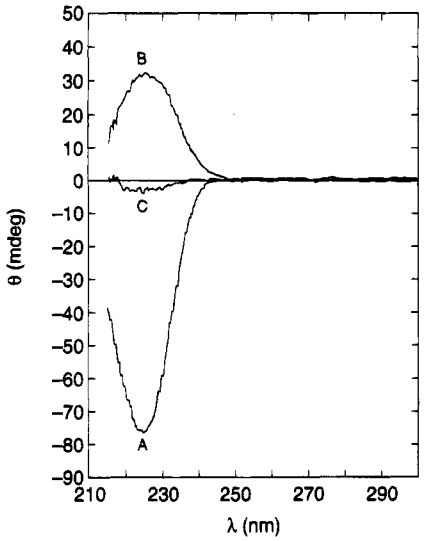

FIGURE 6: Circular dichroic spectra of authentic (*R*)-*p*-(hydroxymethyl)mandelate (A), the *p*-(hydroxymethyl)mandelate produced by the elimination of bromide ion from (*R,S*)-*p*-(bromomethyl)-mandelates in the presence of K166R after 5 min of reaction (B), and racemic *p*-(hydroxymethyl)mandelate (C).

The mechanism of the reaction catalyzed by glutamate racemase recently was examined by Tanner et al. (1993) using an analogous mechanistic approach. The active site of this (metal ion-independent) racemase also has two active site acid/base catalysts that transfer protons to and from the α-carbons of the substrate and product enantiomers. On the basis of sequence alignments (Gallo & Knowles, 1993), both catalysts were proposed to be cysteine residues (Cys 73 and Cys 184). Each cysteine residue was mutated separately to alanine, producing enzymes that were catalytically inactive as glutamate racemases. In analogy to the H297N and K166R mutants of MR, each mutant was able to catalyze the elimination of chloride ion from a single enantiomer of *threo*-3-chloroglutamate, with the stereospecificity being opposite for the two mutants. As a result of these studies, Cys 73 was proposed to function as the (*R*)-specific acid/base catalyst, and Cys 184 was proposed to function as the (*S*)-specific acid/base catalyst.

We conclude that, in the active site of K166R, His 297 retains its ability to catalyze the facile abstraction of the α-proton from (*R*)-*p*-(bromomethyl)mandelate, and, by analogy, (*R*)-mandelate, at a rate that is indistinguishable from the proton abstraction catalyzed by His 297 in the active site of wild-type MR. In contrast, Arg 166 is unable to catalyze the facile abstraction of the α-proton from (*S*)-*p*-(bromomethyl)mandelate, and, by analogy, (*S*)-mandelate. These relative rates can be understood by the structure of the active site of K166R, since the position of the functional group of His 297 is unaffected by the Lys to Arg substitution at residue 166 while the functional group of Arg 166 is necessarily forced to be in an unproductive geometry by steric interactions with the bound substrate.

Conclusions. The high-resolution structure of K166R is the first structure of MR in which a substrate enantiomer is bound in the active site. This structure, like those previously reported for wild-type MR with the inhibitor (*S*)-atrolactate bound in the active site (Landro et al., 1994), wild-type MR inactivated by the affinity label α-phenylglycidate (Landro et al., 1994), and E317Q with the inhibitor (*S*)-atrolactate bound in the active site (Mitra et al., 1995), reveals that the hydroxyl group and one carboxylate oxygen of the substrate are liganded to the essential Mg^{2+}, the metal-coordinated carboxylate oxygen is also hydrogen-bonded to Lys 164, and the other carboxylate oxygen is hydrogen-bonded to Glu 317. The mechanistic studies of the K166R mutant of MR support the previously proposed mechanism (Gerlt et al., 1992) in which Lys 166 functions as the (*S*)-specific acid/base catalyst and His 297 functions as the (*R*)-specific acid/base catalyst. In contrast to the studies previously reported in which Lys 166 was shown to be alkylated by the affinity label α-phenylglycidate and, therefore, implicated in catalysis (Landro et al., 1994), the studies reported in the present paper describe direct measurements of the effects of decreasing the rates of proton transfer to and from the acid/base catalyst of residue 166.

REFERENCES

Brünger, A. T. (1988) *J. Mol. Biol. 203*, 803−816.
Cleland, W. W. (1979) *Methods Enzymol. 63*, 103−138.
Creighton, T. E. (1993) *Proteins: Structure and Molecular Properties*, p 6, W. H. Freeman, New York.
Gallo, K. A., & Knowles, J. R. (1993) *Biochemistry 32*, 3981−3990.
Gerlt, J. A., & Gassman, P. G. (1993a) *J. Am. Chem. Soc. 115*, 11552−11568.
Gerlt, J. A., & Gassman, P. G. (1993b) *Biochemistry 32*, 11943−11952.
Gerlt, J. A., Kenyon, G. L., Neidhart, D. J., Petsko, G. A., & Powers, V. M. (1992) *Curr. Opin. Struct. Biol. 2*, 736−742.
Kabsch, W. (1988a) *J. Appl. Crystallogr. 21*, 67−71.
Kabsch, W. (1988b) *J. Appl. Crystallogr. 21*, 916−924.
Kenyon, G. L., & Hegeman, G. D. (1979) *Adv. Enzymol. Relat. Areas Mol. Biol. 50*, 325−360.
Landro, J. A., Kallarakal, A. T., Ransom, S. C., Gerlt, J. A., Kozarich, J. W., Neidhart, D. J., & Kenyon, G. L. (1991) *Biochemistry 30*, 9274−9281.
Landro, J. A., Gerlt, J. A., Kozarich, J. W., Koo, C. W., Shah, V. J., Kenyon, G. L., Neidhart, D. J., Fujita, S., & Petsko, G. A. (1994) *Biochemistry 33*, 635−643.
Lin, D. T., Powers, V. M., Reynolds, L. J., Whitman, C. P., Kozarich, J. W., & Kenyon, G. L. (1988) *J. Am. Chem. Soc. 110*, 323−324.
Mitra, B., Kallarakal, A. T., Kozarich, J. W., Gerlt, J. A., Clifton, J. G., Petsko, G. A., & Kenyon, G. L. (1995) *Biochemistry 34*, 2777−2787.
Neidhart, D. J., Howell, P. L., Petsko, G. A., Powers, V. M., Li, R., Kenyon, G. L., & Gerlt, J. A. (1991) *Biochemistry 30*, 9264−9273.
Ransom, S. C., Gerlt, J. A., Powers, V. M., & Kenyon, G. L. (1988) *Biochemistry 27*, 540−545.
Sambrook, J., Fritsch, E. F., & Maniatis, T. (1989) *Molecular Cloning: A Laboratory Manual*, Cold Spring Harbor Laboratory Press, Cold Spring Harbor, NY.
Sharp, T. R., Hegeman, G. D., & Kenyon, G. L. (1979) *Anal. Biochem. 94*, 329−334.
Tanner, M. E., Gallo, K. A., & Knowles, J. R. (1993) *Biochemistry 32*, 3998−4006.
Tronrud, D. E. (1992) *Acta Crystallogr. A48*, 912−916.
Tronrud, D. E., Ten Eyck, L. F., & Matthews, B. W. (1987) *Acta Crystallogr. A43*, 489−501.
Tsou, A. Y., Ransom, S. C., Gerlt, J. A., Powers, V. M., & Kenyon, G. L. (1989) *Biochemistry 28*, 969−975.
Whitman, C. P., Hegeman, G. C., Cleland, W. W., & Kenyon, G. L. (1985) *Biochemistry 24*, 3936−3942.

BI9419893